White paper

qCMOS®: Quantitative CMOS technology enabled by Photon Number Resolving

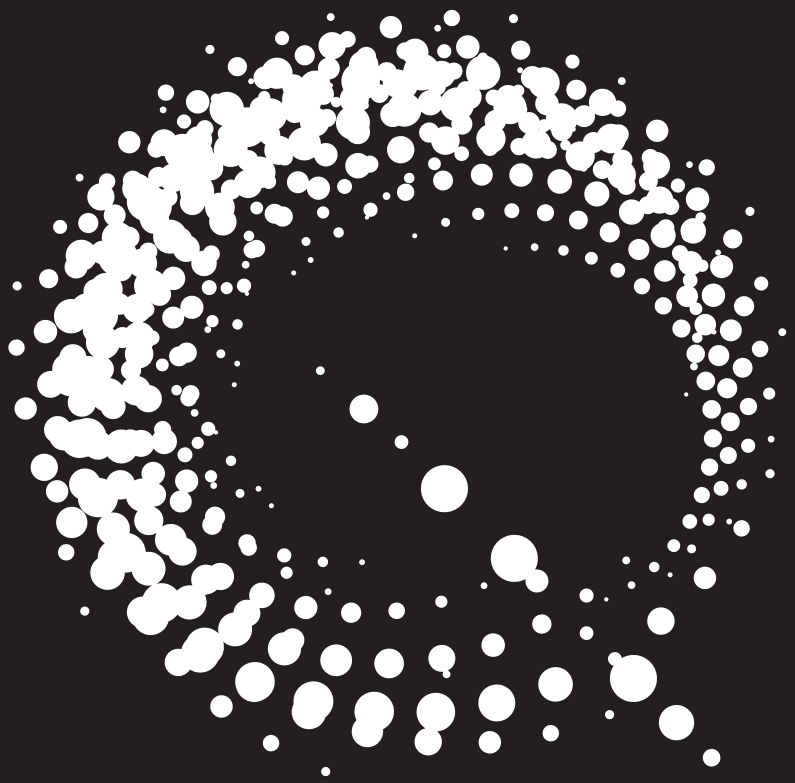

HAMAMATSU

PHOTON IS OUR BUSINESS

Table of Contents

Introduction

In the early 1900s, physicists were struggling with the explanation of two crucial optical phenomena: The emission of light from a hot object (blackbody radiation), and the release of detectable charge from a metallic surface under illumination (photoelectric effect). The breakthrough came when Max Planck and Albert Einstein took a drastic step: They postulated that light is quantized [1]. This created quite a stir because, according to Einstein, light is not a continuous stream of energy transported by waves; rather it is a drumfire of energetic particles! Today we know that Einstein was right, and we call these light particles photons.

In 1921, Albert Einstein deservedly received the Nobel Prize for his seminal work on the true nature of light as a torrent of photons.

The consequences of the fact that light consists of particles are enormous. In particular, because it implies that there exists a lower limit to the detection of electromagnetic radiation: If we can resolve the arrival of a single photon, we have reached the fundamental detection limit of light. Thanks to the relentless progress of semiconductor technology and to the development of clever electronic circuitry for the detection of photogenerated charge, it has finally become possible to fabricate megapixel image sensors and cameras, capable of reaching this ultimate, photon number resolving limit.

This White Paper explains the different approaches, properties and shortcomings of a photon number resolving camera based on semiconductor technology.

1. Principle of Semiconductor Image Sensor

1.1 From photons to photocharges, and to image data

Many of the properties of semiconductor image sensors and the various approaches to realize photon number resolving can be understood by considering the different physical effects occurring in an image sensor. Fig. 1-1 shows a cross-section through a typical image sensor. Today, most are fabricated on a silicon substrate, making use of the ubiquitous CMOS (Complementary Metal-Oxide Semiconductor). An image sensor can be illuminated from the front, where the electronic circuitry was fabricated, or for best performance it is illuminated from the back; this situation is illustrated in Fig. 1-1.

The backside of such an image sensor is covered by a protective, anti-reflection coating 1. At the back of the image sensor – which was the front during processing – the pixel structures for electronic photocharge detection 4 are situated.

Electronic signals are transported to electronic signal processing circuits 5, then amplified, processed and conditioned so that they can be read out from the chip at the output 6 without additional loss of performance. The interior of the semiconductor consists of two regions: Close to the pixel structures, an electric field can be felt. In this field region 3 charge will be transported along the electric field lines to the individual pixels. In the field-free region 2 – also called diffusion region – charges will diffuse randomly in all directions, until they either recombine without ever being detected, or they reach the field region 3 where they are quickly moved to the pixel structures in 4.

The individual pixels are not separated from each other by mechanical walls. Rather, the electric field in the field region 3 is responsible for the “virtual pixel boundaries” 7. The electric field lines are engineered such that mobile charges cannot move laterally but they are rather transported straight to the corresponding pixel.

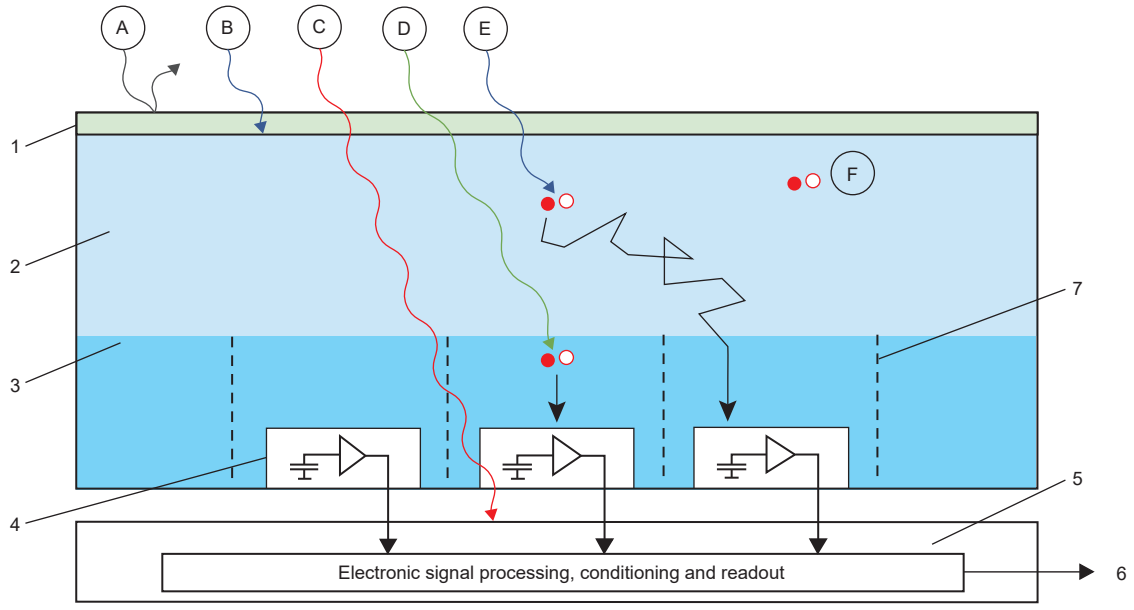

Fig. 1-1 Cross section through a semiconductor image sensor, illustrating the different physical effects influencing the detection performance of such an imaging system.

1 Protective layer on the top surface of the image sensor;
2 Field-free region (Diffusion region);
3 Electric field region;
4 Pixel structures for electronic photocharge detection;
5 Electronic signal processing circuits (column amplifiers, low-pass filters, pixel addressing, etc.);
6 Off-chip readout of image sensor signals;
7 Virtual pixel boundaries created by electric fields near the image sensor’s bottom surface;

There are five fundamental ways in which incident photons can interact with a semiconductor image sensor.

In process A, an incident photon is just reflected off the protecting surface layer 1 without ever entering the image sensor. The effect of this process can be minimized by fabricating optical anti-reflection multi-layer coatings on top of the surface layer 1.

In process B, an incident photon is absorbed in the surface layer 1, and no electronically detectable event results. This happens predominantly with higher-energy (UV and blue) photons, explaining the fact that the sensitivity of silicon image sensors is reduced towards shorter wavelengths.

In process C, an incident photon travels unimpededly through the image sensor. Since it does not interact with the semiconductor in its sensitive regions 2 or 3, such a photon cannot be detected. This happens predominately with lower-energy (infrared) photons, explaining why the image sensors' sensitivity is reduced towards longer wavelengths.

In process D, an incident photon interacts with the semiconductor in the field region 3. This creates a pair of mobile photo-charges, an electron (illustrated as a full circle in Fig. 2) and a hole (illustrated as an open circle). The free electron is transported along the electric field lines straight to the electronic charge-detection circuity in the corresponding picture. The free hole moves in the opposite direction, and it finally recombines with an electron in the field-free region 2.

In process E, an incident photon interacts with the semiconductor in the field-free region 2, creating a pair of photo-charges diffusing randomly in all directions. As mentioned above, this undirected movement only stops if the charge carriers recombine after a certain time (the so-called recombination time) in the field-free region 2, or if the photoelectron reaches the boundary of the field region 3. Once this has happened, the photoelectron is transported straight to the corresponding pixel for electronic charge detection. However, due to the random motion from the interaction location to a pixel, positional information is lost. Therefore, the farther away the creation of a charge pairs happens from the field region 3, the more diffuse and spread-out is the resulting picture.

Finally, the often-neglected process F needs to be discussed. Although it is true that a photon can only interact with a semiconductor if the photon's energy is large enough (essentially larger than the semiconductor's bandgap energy), a mobile charge pair can also be created without the intervention of a photon: The necessary energy for the charge pair creation can be supplied by thermal energy, i.e. sufficiently strong semiconductor lattice vibrations. This is the origin of the dark current, which is exponentially increasing with temperature.

Despite the loss processes A, B and C described above, the creation of photo-charges in semiconductors is a very efficient process. The performance of the photodetection is measured with the parameter Quantum Efficiency (QE), measuring the fraction of photo-generated and electronically detectable charge pairs per incident photons. A QE of 100 % implies, therefore, that each incident photon creates one electronically detectable electron-hole pair. In modern semiconductor image sensors, a QE of close to 100 % is reached at intermediate (often visible) wavelengths, while there is a roll-off of the QE towards longer (infrared) and shorter (blue, UV) wavelengths.

Despite the excellent QE of semiconductor image sensors, their performance is limited by physical processes that introduce noise into the detection process.

1.2 Noise sources in semiconductor photosensors

There are three main sources of noise that are limiting the performance of semiconductor photosensors [2].

(1) Readout noise (σ_R), i.e. the statistical uncertainty of the electronic photocharge detection process, which depends on the electronic circuit's bandwidth, on the temperature, and most importantly on the effective capacitance at the input of the photo-detection circuit

(2) Dark current noise (σ_D), i.e. the statistical variation of the dark current, which is increasing exponentially with temperature

(3) Photon shot noise (σ_P), i.e. the statistical variation in the number of incident photons

1.2.1 Readout noise (σ_R)

The first major contributor to noise of an image sensor is the statistical uncertainty in the electronic charge detection process. Noise in the electronic circuit's first transistor prevents a noise-free measurement of the photocharges. This is illustrated in a simplified way in Fig. 1-2: In many cases, the electronic circuit consists of a voltage follower, where a change in input voltage creates the same voltage change at the output. At the circuit's input, the effective capacitance C is present. When the photocharge Q is placed on this capacitance, a proportional voltage increase V is observed:

$$V = \frac{1}{C}\,Q \qquad (1\text{-}1)$$

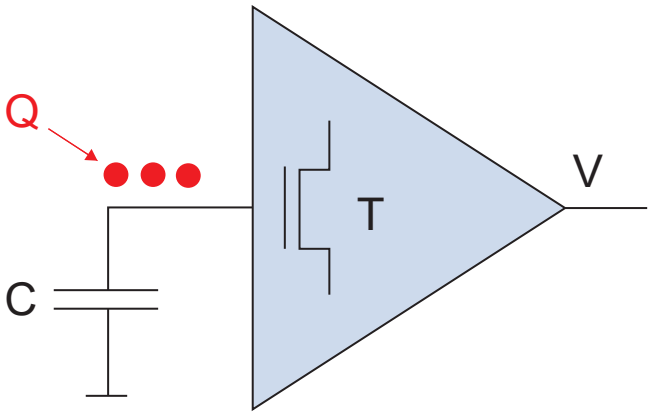

Fig. 1-2 Principle of electronic photocharge detection: The photocharge Q is placed on the effective input capacitance C, creating a voltage response V = Q/C

If just one electron (one unit charge q = 1.602×10^{-19} As) is placed on the input capacitance C, the voltage increase is equal to q/C. This proportionality constant S = q/C is called the "charge detection sensitivity" or "conversion gain" of the charge detection circuit. As an example, consider an effective input capacitance C of 1.6 fF. In this case, the charge detection sensitivity of the charge detection circuit is 100 µV/electron.

The first transistor T in the electronic photocharge detection circuit exhibits thermal noise. For this reason, the output voltage V is also noisy. As a consequence, the measurement of the charge Q at the circuit's input, determined using equation (1-1), is also exhibiting thermal noise. The standard deviation σ_Q of the electronic photocharge detection process essentially depends on the effective input capacitance C, the absolute temperature T and the circuit's measurement bandwidth B. It is approximately given by the proportionality.

$$\sigma_Q \propto C\sqrt{B\,T} \qquad (1\text{-}2)$$

This noise is typically measured in electrons as $\sigma_R = \sigma_Q/q$, and it is called "readout noise".
It is immediately evident from equation (1-2) what needs to be done to reduce the readout noise in an image sensor: On one hand, the bandwidth B needs to be reduced significantly. This is achieved by providing each column of the image sensor with its own low-pass filter, so that the effective bandwidth B for reading out a pixel is not measured in tens of MHz as in CCD image sensors, but rather in tens of kHz. This is the fundamental reason why the performance of today's CMOS image sensors is superior to the performance of the best CCD image sensors. This is explained in detail in chapter 2.

On the other hand, reducing the effective input capacitance C is the other major factor for diminishing the readout noise. Thanks to the relentless progress of semiconductor technology, the minimum feature size in electronic circuits is shrinking continuously. Thus, the size of the pixels and their effective capacitances C are also shrinking. As an example, consider the record-low-noise pixels described in Reference [3]. This was achieved by reducing the effective capacitance to 0.464 fF, corresponding to a charge detection sensitivity S = 345 µV/electron. In this way, a readout noise of only about 0.23 electrons rms at room temperature was attained.

1.2.2 Dark current noise (σ_D)

A second source of noise in a photosensor is the dark current. Thermal excitation of mobile electron-hole pairs is adding a signal that is indistinguishable from the signal created by the incident photons. The dark current density j depends on the absolute temperature T and the bandgap energy E_g of the semiconductor, and it can be approximated by the following proportionality [4]:

$$j \propto T^{\frac{3}{2}} e^{-\frac{E_g}{2kT}} \quad (1\text{-}3)$$

with Boltzmann's constant k = 1.3807×10^{-23} J/K. The proportionality constant in equation (1-3) depends on the quality, the doping and the volume of the semiconductor contributing to the dark current.

The almost exponential relationship of equation (1-3) is illustrated in Fig. 1-3 in the case of silicon, exhibiting a bandgap energy E_g of about 1.2 eV:

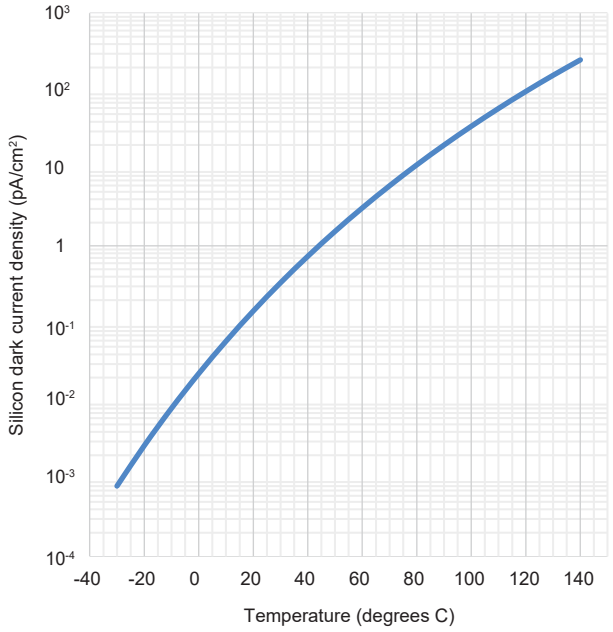

Fig. 1-3 Dark current density as a function of temperature, as described by equation (1-3) for the case of high-quality silicon

The graph also illustrates the well-known rule of thumb that in silicon the dark current density is halved with each reduction of the temperature by about 8 °C, provided that the device is operated not too far from room temperature.

The dark current density j is typically measured in pA/cm², as indicated also in Fig. 1-3. From this the dark count rate (DCR) of a pixel with an area A can be calculated:

$$DCR = \frac{j\,A}{q} \quad (1\text{-}4)$$

As an example, consider the dark current density shown in Fig. 1-3 at room temperature (20 °C), which is about 0.15 pA/cm². Assuming a pixel area of 4.6×4.6 µm² and employing equation (1-4), a DCR = 0.2 electrons/pixel/s can be calculated.
Also the total dark current (DC) is calculated by multiplying it with the exposure time (T).

$$DC = DCR \times T \quad (1\text{-}5)$$

Since the dark current is an additive component to the total current flowing to a pixel, it is possible to cancel its contribution by simply measuring it (capping the lens to keep the image sensor in the dark for calibration) and by subsequent subtraction of the dark signal from each corresponding pixel signal. This processing effectively removes the dark current contribution from the photosignal, but it cannot remove the contribution of the dark current noise to the total signal noise. The flow of a dark current corresponds to the independent transport of charge carriers, and this is a random process with a Poisson distribution (also see 1.2.3). As a consequence, the flow of the dark current is a noisy process exhibiting a standard deviation given by

$$\sigma_D = \sqrt{DC} \quad (1\text{-}6)$$

This σ_D is called "dark current noise" and this noise contribution has to be taken into account when determining the total noise performance of an image sensor.

Let's use the value of the dark count rate calculated above, DCR = 0.2 electrons/pixel/s, for a practical example: Assuming an exposure time of 100 seconds, this dark current contributes an average number of 20 electrons to the pixel signal. This number can be subtracted from each pixel signal, so that the corrected signal corresponds exclusively to the number of detected photoelectrons. However, the Poisson noise of the dark current of √20 = 4.5 electrons rms represents a significant addition to the total signal noise. The only way to reduce the dark current noise is to decrease the dark current itself. This is possible by cooling the image sensor. As shown in Fig. 4, cooling to -30 °C reduces the dark current density to 0.8 fA/cm² in this example, corresponding to a dark current rate of only 0.001 electrons per second on average. During the exposure time of 100 seconds mentioned above, the dark current contributes therefore only 0.1 electrons to the pixel signal on average.

1.2.3 Photon shot noise (σ_P)

Most of the light sources that are commonly used in optical systems, including stabilized single-mode lasers, LEDs, incandescent light sources and discharge lamps, exhibit a Poisson distribution in the photon number they are emitting [2]. This is called "photon shot noise". If a source of particles (e.g. photons or electrons) is emitting these particles randomly and independently of each other, the source is exhibiting a Poisson probability distribution: The probability $P_N(k)$ of finding k particles during a given observation time, for which an average number N of emitted particles is seen, is given by

$$P_N(k) = \frac{N^k \, e^{-N}}{k!} \qquad (1\text{-}7)$$

As an example, the Poisson distribution for the case N = 7 is shown in Fig. 1-4.

The Poisson distribution has the important property that the standard deviation σ_P is equal to the square root of the average particle number N, i.e.

$$\sigma_P = \sqrt{N} \qquad (1\text{-}8)$$

and this σ_P is called "photon shot noise".
The larger the average particle number N is, the closer the Poisson distribution becomes to a Gaussian distribution for which the square root law of equation (1-8) holds true for the standard deviation.

As mentioned above, most light sources exhibit shot noise, i.e. a Poisson distribution of their photon numbers. In actual optical systems, many of a light source's photons are lost due to optical apertures, filters, diffusers, beam splitters, absorbers or diffractive elements. A final important signal loss occurs during the incomplete conversion of photons into photogenerated charge pairs in an image sensor, with a QE that can be significantly below 100 % for certain wavelengths.

The question, therefore, is how the original Poisson distribution of the system's light source is modified by the various losses. The answer is surprisingly simple and immensely practical: Assume a Poisson-distributed source of particles and a physical selection process decimating the particle numbers. Some particles are left, and others are removed from the incoming stream. If this selection process is completely random, then the distribution of the decimated particles is, again, Poisson.

As a consequence, the loss of photons from a Poisson-distributed light source (through absorption, scattering, beam-splitting, filtering, diffraction, etc.) produces, again, a Poisson-distributed light source. And the conversion of a Poisson-distributed stream of incoming photons in an image sensor, produces a Poisson-distributed number of photogenerated charge carriers, irrespective of the properties of the QE curve. Obviously, the Poisson distribution is ubiquitous!

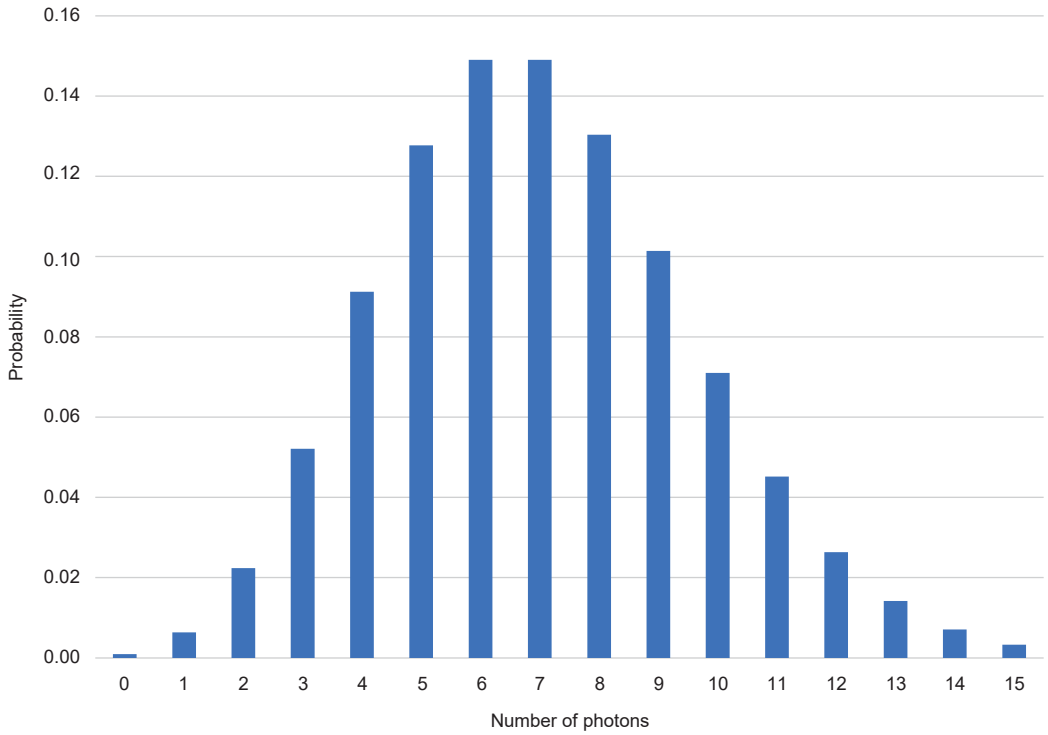

Fig. 1-4 Poisson-distributed probability $P_N(k)$ of observing a number k of particles (e.g. photons) during a certain observation time for which an average number of N = 7 particles is observed

1.3 Dynamic range D/R, signal-to-noise SNR and relative signal-to-noise rSNR

The noise sources described in the previous sections are often employed to calculate figures of merit for image sensors and cameras, so that their performance can be compared. A first parameter is the dynamic range D/R, making use of the maximum charge N_{max} that can be detected by the electronic circuit. N_{max} is often called Full Well Capacity of the image sensor's pixels. D/R compares the full well capacity with the readout noise according to section (1.2.1),

$$D/R = \frac{N_{max}}{\sigma_R} \qquad (1\text{-}9)$$

As an example, consider an image sensor with a full well capacity of N_{max} = 5000 electrons and a readout noise of σ_R = 0.5 electrons rms. According to equation (1-9), the dynamic range of this image sensor is D/R = 5000/0.5 = 10 000:1.

An even more important parameter is the signal-to-noise ratio SNR. It is based on the assertion described in the previous sections that the total noise of an image sensor consists of three different noise sources: Photon shot noise σ_P, dark current noise σ_D and readout noise σ_R. Since these three noise sources are statistically independent, the total noise σ is given by

$$\sigma = \sqrt{\sigma_P^2 + \sigma_D^2 + \sigma_R^2} = \sqrt{N + M + \sigma_R^2} \qquad (1\text{-}10)$$

assuming that the average number of detected photoelectrons is N and the average number of dark current generated electrons is M, and making use of the fact that both parameters are Poisson-distributed. According to equation (1-10), SNR is therefore defined as

$$SNR = \frac{N}{\sigma} = \frac{N}{\sqrt{N+M+\sigma_R^2}} = \frac{S \times QE}{\sqrt{S \times QE + M + \sigma_R^2}} \qquad (1\text{-}11)$$

where we have made use of the fact that the average number of photons S incident on a pixel during the exposure time is related to the average number of photo-generated electrons N through the quantum efficiency QE, i.e. N = S×QE [5].

It is interesting to compare the noise performance of a camera with the ideal case of pure Poisson noise. This can be done with the 'relative SNR' value, defined as the ratio between the actual SNR value and pure Poisson noise $\sigma_i = \sqrt{S}$:

$$rSNR = \frac{SNR}{\sigma_i} = \frac{SNR}{\sqrt{S}} \qquad (1\text{-}12)$$

One could argue that this is a comparison of an actual camera exhibiting a certain SNR, with the SNR of an ideal camera showing a QE of 100 %, no dark current and no readout noise [5].

In Fig. 1-5 the rSNR behavior of a camera with a QE of 80 %, a readout noise of σ_R = 1.0 electrons rms and a dark count of M = 2.0 electrons is shown. As is obvious from equations (1-11) and (1-12), the asymptotic value of a camera's rSNR is given by $\sqrt{QE}$; in the present case this is $rSNR_{asympt}$ = 0.894.

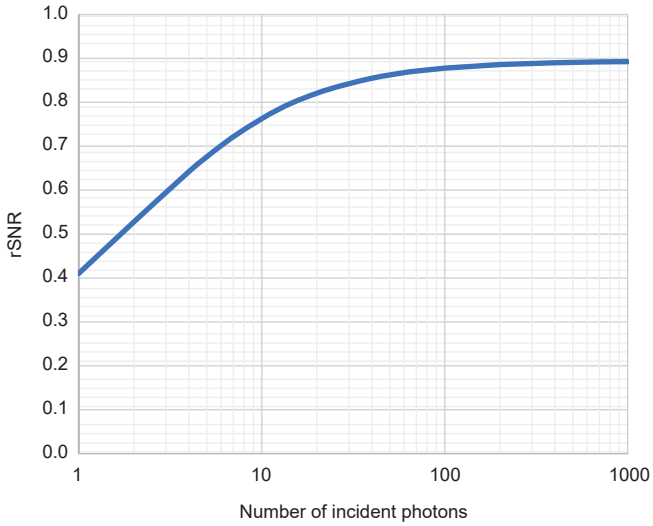

Fig. 1-5 rSNR as a function of photon number S for a camera with a QE of 80 %, a readout noise of σ_R = 1.0 electrons rms and a dark count of M = 2.0 electrons.

Light consists of energetic particles – photons – which can be individually detected in the pixels of semiconductor image sensors. Not all incident photons can interact with the semiconductor material and produce an electronically detectable charge: High-energy photons are predominantly absorbed at the surface of the image sensor, while low-energy photons are transmitted unimpededly through the image sensor.
Three main noise sources reduce the precision with which light can be detected in a semiconductor image sensor: (1) Readout noise in the pixels' first transistor channels, (2) Dark current noise depending exponentially on temperature, and (3) Photon shot noise due to the Poisson distribution of photon numbers in most common light sources.
In today's most advanced CMOS image sensors, a readout noise of 0.2 to 0.3 electrons rms at room temperature is achieved by using small transistor geometries with sub-fF effective input capacitances and circuit bandwidths of a few 10 kHz. By employing high-quality semiconductor material and by cooling, dark counts of less than 1/1000 electrons per second and per pixel can be attained.
The performance of different cameras can be compared with suitable figures of merit and graphics, such as the dynamic range (D/R), signal-to-noise ratio (SNR) and the relative signal-to-noise ratio (rSNR).

2. State-of-the-Art Approaches to Quantitative Semiconductor Image Sensors

In the early 1940s silicon was considered as one of the potentially interesting materials for electronic applications. The huge potential of semiconductors and of silicon was first realized at the famous Bell Labs, when Russell Ohl observed to his surprise that a special piece of silicon was sensitive to light [6]. Without knowing it, the technologists had manufactured a diode, which also acted as a photodiode. It was therefore realized early on that photosensors and image sensors can be fabricated with silicon. Although the driving force in the relentless progress of semiconductor manufacturing was integrated microelectronics, the image sensor has always profited immediately from the progress in production, the shrinking minimum feature sizes, the rising level of integration and the rapidly falling prices.

2.1 Architectures and Evolution of Semiconductor Image Sensors

The more optoelectronic functionality possible in each pixel and on each image sensor, the higher the performance of the resulting image sensors. The different architectures of image sensor and the evolution of the various generations of the image sensor are illustrated in Fig. 2-1:

The simplest semiconductor image sensor consists of a two-dimensional array of pixels, each of which contains a photodiode and a transistor switch. Such a photodiode array (PDA) is illustrated in Fig. 2-1(a). Each column is connected with its correct switch to the single output amplifier. By properly setting the pixel and column switches, one pixel at a time can be connected to the single readout amplifier. PDA products were popular in the 1960s, despite their rather high readout noise. This is easily understood when considering the noise contributed by the first transistor in the readout amplifier. The effective capacitance at the amplifier's input is several pico-Farads, due to the long electric lines and the many switches on these lines. According to equation (1-2), readout noise is directly proportional to the effective capacitances, and it is therefore no surprise that the readout noise of these PDAs could be as high as a few 1000 electrons rms. The invention of the Charge Coupled Device (CCD) principle in 1969 brought a huge reduction of the readout noise.

As illustrated in Fig. 2-1(b), this is achieved by shifting the photogenerated charges from the photosensitive 2D area row by row into a one-dimensional readout register. For each row, the photo-charges are moved one by one to the output amplifier. In this way, the effective capacitance at the input of the readout amplifier can be reduced substantially. As a consequence, the readout noise was decreased by one or two orders of magnitude to 10 to 100 electrons rms. Also, by slowing down the readout speed, it was possible to reduce the readout noise to below 10 electrons rms.

In addition to decreasing the readout noise, the QE was also improved to around 70 % at peak by adopting microlenses on the image sensor. Still, in some applications of fluorescence microscopy imaging, the number of photons returned from the sample was too small to acquire useful imagery, not even with a camera offering lower readout noise and higher QE. For such applications, long exposure time imaging with a low dark current camera employing sensor cooling was necessary. This was the reason why the cooled CCD camera (ORCA® C4742-95 series) from Hamamatsu Photonics, was a major tool for this application from 1990s to 2000s.

The situation of PDAs changed dramatically with the realization that the first transistor of an electronic photodetection circuit could be placed in each pixel, as illustrated in Fig. 2-1(c).The consequence was that the effective capacitance at the transistor's gate was as small as in the CCD image sensor. However, since regular photodiodes can be employed, such an APS (Active Pixel Sensor) can be produced with a standard CMOS process and does not need a special CCD manufacturing process [7]. A second advantage of employing CMOS technology is the possibility to reduce the bandwidth of the photo-charge measurement.

As indicated in equation (1-2), the readout noise depends on the square root of the bandwidth. Therefore, each column of the CMOS image sensor is supplied with its own low-pass filter (LPF) circuit, so that the time needed to read out a complete line can be employed for low-pass filtering of the pixel signal selected by the pixel switch, thus reducing the readout noise in CMOS image sensors even further – ultimately below the limit possible with CCD technology.

This started the revolution of CMOS image sensor in the early 1990s, with cost-effective CMOS image sensors exhibiting similarly low readout noise values of 10 to 100 electrons rms as the CCD image sensors of the time.
Despite the revolution of the CMOS image sensor, CCD cameras were preferred from the 1990s to 2000s in scientific applications, because the CMOS image sensors had a problem with pixel uniformity.

The implementation of individual photodetection circuits in each pixel brought pixel variations of gain and offset, and due to those variations the image quality of CMOS image sensors was not as good when compared with CCD sensors.

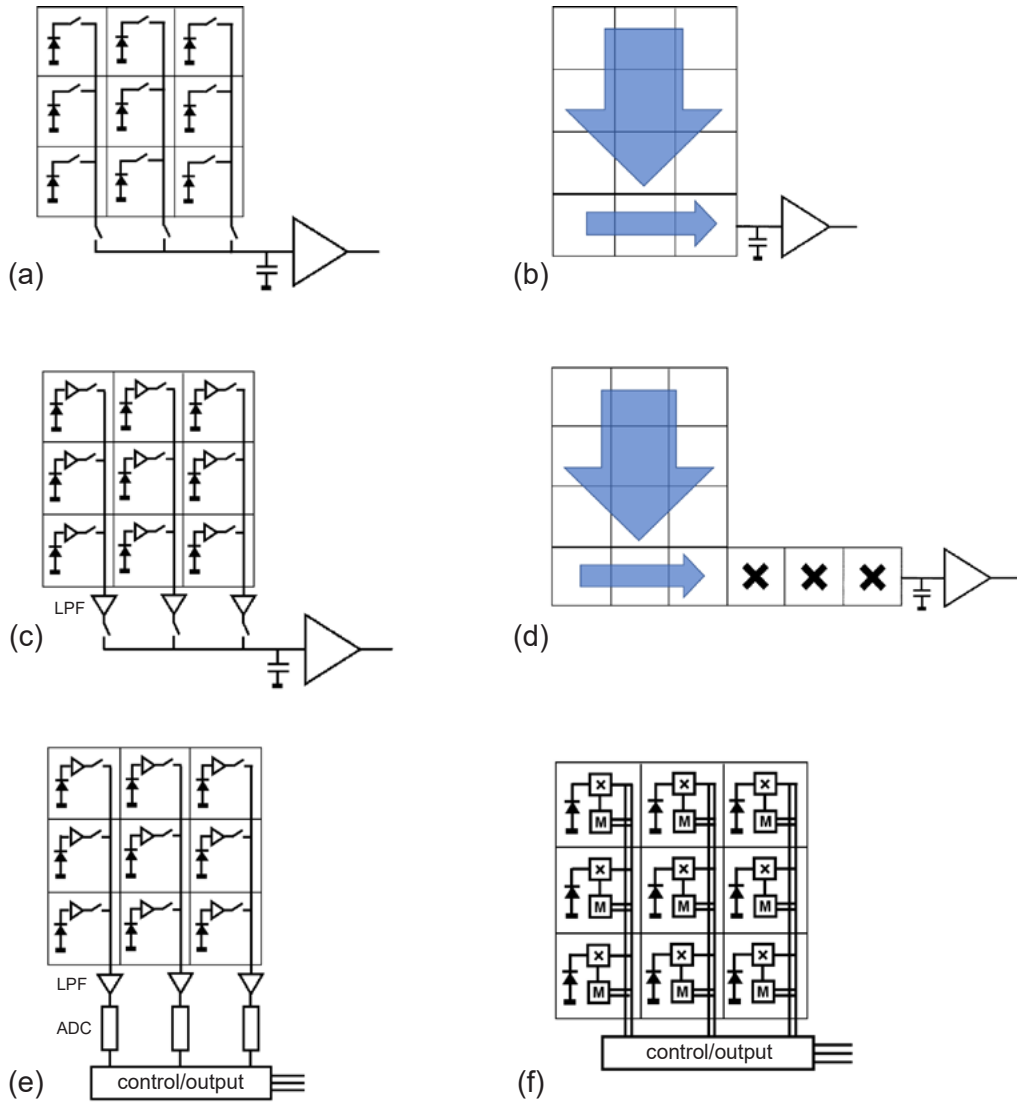

Fig. 2-1 Architectures and evolution of semiconductor image sensors: (a) Photodiode array, (b) Charge-Coupled Device (CCD) image sensor, (c) CMOS/APS (Active Pixel Sensor) image sensor (Generation I CMOS), (d) CCD image sensor with avalanche multiplication register, (e) sCMOS (scientific CMOS) image sensor, (f) APD and SPAD array (Single Photon Avalanche Diode)

2.2 EM-CCD (Electron-Multiplying Charge Coupled Device)

The problem to be solved is that the noise contribution of the photodetection circuit is much larger than the one electron that is produced through the interaction of one photon with the semiconductor material.

Our photodetection task would be much easier if we had larger charge packets to detect.
Fortunately there exists a physical charge multiplication mechanism that provides exactly the sought functionality – it is called the avalanche effect. It is based on the assertion that in a semiconductor a free electron-hole pair can be generated through the introduction of a sufficient amount of energy

(essentially larger than the semiconductor's bandgap energy). The solution is surprisingly simple: If we apply a high enough electric field, one mobile electron will be converted into more electrons. Although this process introduces "multiplication noise", it can be advantageous to work only with small multiplication factors but to apply such small multiplication several times in series. This is the basic idea behind the EM-CCD (Electron-Multiplying CCD), which is also known as "Impactron" [8].

As illustrated in Fig. 2-1(d), an EM-CCD image sensor consists of a regular CCD image sensor with an additional "multiplication register". This is a linear CCD structure where higher voltages can be applied, so that each charge shift introduces also a small multiplication of the transported charge packet. The effect is that one photogenerated electron can therefore be converted into a charge packet containing several ten or hundred electrons. Detecting these multiplied charge packets with a conventional CCD charge detection circuit is simple because the circuit's readout noise is small compared with the size of the amplified charge packet.

During the 2000s, EM-CCDs were produced with an effective readout noise of less than one electron rms. In this way semiconductor cameras offering single-photon detection became possible for the first time, such as the ImagEM® (C9100-13) from Hamamatsu Photonics.

Although EM-CCDs offer single-photon detection capability, they do not have photon number resolving capability because of "multiplication noise" which adds noise to the photoelectron signal.

There is another image sensor technology employing avalanche multiplication called "SPAD (Single Photon Avalanche Diode)". SPAD technology offers single-photon detection capability by using electron multiplication in each pixel, as illustrated in Fig 2-1(f). SPAD arrays are mainly used to obtain high temporal resolution (typically of the order of several tens of picoseconds) and they have some disadvantages for imaging such as the small pixel number, the restricted dynamic range and the low QE.

2.3 sCMOS (Scientific CMOS)

The relentless progress of CMOS technology made it possible to reduce the size of the transistors and pixels in the 2000s – and therefore to reduce the value of the effective capacitance at the gate of the first transistor. At the same time, it was also possible to co-integrate more digital functionality on the image sensor chip, in particular analog-to-digital converters (ADC). As illustrated in Fig. 2-1(e), each column obtained its own ADC circuit which enabled parallel ADC processing. Thanks to this parallel processing, the charge readout bandwidth could be reduced by employing low-pass-filters LPF, and the readout noise was also reduced, as shown in equation (1-2). As a result, readout noise values of 1 to 3 electrons rms were realized with such CMOS image sensors, and this sensor type was called "Scientific CMOS (sCMOS)", indicating its high performance as required for scientific grade applications.

2.4 Generation II sCMOS

Despite offering low noise, first generation sCMOS image sensors were not well accepted in scientific applications because of their relatively low QE compared with CCD image sensors. In the case of CMOS image sensors, several transistors are required in each pixel for electronic photodetection and switching, thus reducing the photo-sensitive area (photodiode area). As a result, the peak QE of first generation sCMOS image sensors were limited to 55 % even when using microlenses over each photodiode.

To overcome this situation, the QE of sCMOS image sensors were increased by optimizing the number of transistors, leading to 72 % at peak QE, which was competitive to CCD image sensors. These types of sCMOS image sensors with improved QE were called "Generation II sCMOS (Gen II sCMOS)".

In 2011 Hamamatsu Photonics released the ORCA®-Flash4.0 camera (C11440-22CU), which adopted Gen II sCMOS. It achieved both low readout noise (1.6 electrons rms) and high QE (72 %). Also, thanks to the progress of image processing components (for example, FPGAs), the image quality of sCMOS cameras were dramatically improved by implementing real-time image correction algorithms directly in the camera.

Because of these achievements the ORCA®-Flash4.0 was widely adopted in scientific applications, rapidly spreading and replacing CCD cameras.

This development effort was continued, leading to sCMOS cameras with improved QE and reduced readout noise. This was achieved by optimizing the microlenses and by applying a slow-scan mode. The peak QE and the readout noise of the latest Gen II sCMOS, which is adopted in the ORCA®-Flash4.0 V3 (C13440-20CU), are 82 % and 1.4 electrons rms, respectively.

2.5 Generation III sCMOS

Regarding the readout noise of CMOS image sensors, including Gen II sCMOS, one special issue needs to be highlighted: Ideally the characteristic of readout noise for each pixel should be same. However, pixel-to-pixel readout noise variations are observed because each pixel has its own photodetection circuit. Fig 2-2 shows the typical noise distribution of Gen II sCMOS. It is obvious that there are certain pixels whose readout noise is larger than 5 electrons (which is about 3 times larger than the rms value and 6 times larger than the median value). Those pixels lead to visually dark and bright spots, which is called “salt and pepper noise” (illustrated in Fig 2-3), that also affect quantitative measurements.

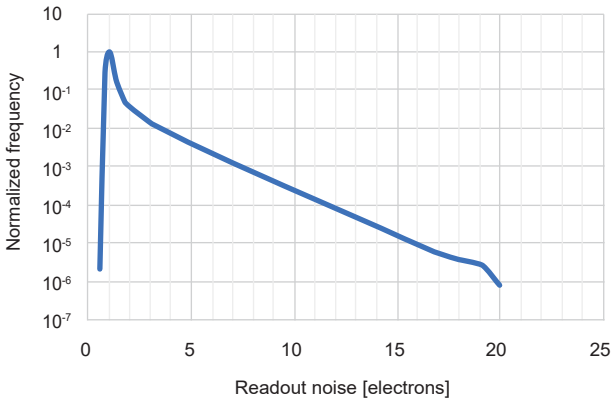

Fig 2-2 Typical noise distribution of Gen II sCMOS

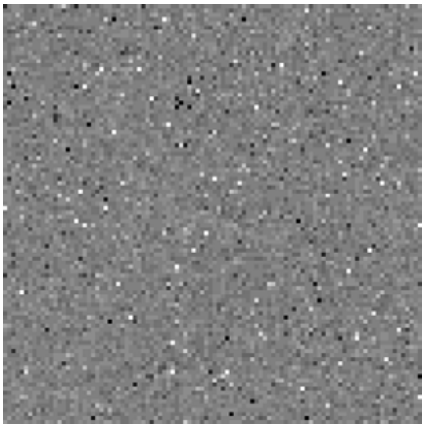

Fig 2-3 Salt and pepper noise

As a consequence, Hamamatsu Photonics developed a new type of scientific CMOS image sensor to improve this readout noise issue. By optimizing the transistor design and the semiconductor process employed for the fabrication of the photodetection circuits, the readout noise variations were reduced dramatically, as shown Fig 2-4. This noise-improved type of sCMOS image sensor is called “Generation III sCMOS (Gen III sCMOS)”.

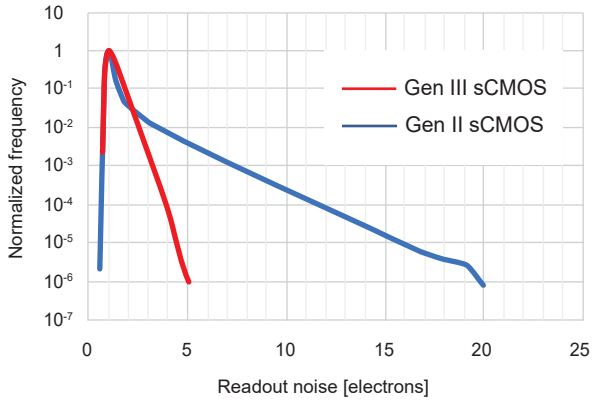

Fig 2-4 Comparison of typical noise distributions between Gen II sCMOS and Gen III sCMOS

In 2018 Hamamatsu Photonics released the ORCA®-Fusion camera (C14440-20UP) which adopted Gen III sCMOS. This was the first camera to realize less than 1 electron rms readout noise (0.7 electrons rms at ultra-quiet mode) employing sCMOS image sensor technology.

In addition, in 2020, Hamamatsu Photonics released their latest camera, the ORCA®-Fusion BT (C15440-20UP) which adopted Gen III sCMOS with BSI (Back-Side Illumination) technology.

Image sensor type	Predominant use period	Pixel number (pixels)	Frame rate (fps)	Peak QE (%)	Readout noise (electrons rms)	Multiplication noise
CCD	1990s to 2000s	1344 × 1024	16.2	70 %	6	No
EM-CCD	2000s to 2010s	512 × 512	32	97 %	< 1	Yes
Gen II sCMOS	2011 to 2020	2048 × 2048	100	82 %	1.4	No
Gen III sCMOS	2018 until today	2304 × 2304	89.1	95 %	0.7	No

Table 2-1 Main image sensor types which have been used in scientific applications

3. qCMOS® : Quantitative CMOS Image Sensor

When reading about the impressive progress in semiconductor image sensors described in the previous Chapter, one might think that Gen III sCMOS image sensors and cameras have attained our original goal: With a readout noise of 0.7 = electrons rms it should be possible to detect individual incident photons. Well, is it?

The question can be answered by looking at a typical distribution of the photoelectron detection signal of an image sensor. Let us assume that the probability distribution of the photoelectron number is a Poisson distribution, as described in equation (1-7), with mean photoelectron number N = 3. Since each photocharge measurement is affected by the statistical uncertainty of the readout noise σ_R, according to the proportionality (1-2), only a "blurred" Poisson distribution of the photoelectrons can be observed. This is illustrated in Fig. 3-1 for three values of the (Gaussian) readout noise: σ_R = 0.5 electrons (blue curve), σ_R = 0.3 electrons (red curve), and σ_R = 0.15 electrons (green curve).

It is obvious from Fig. 3-1 that it is impossible to distinguish between the various photoelectrons if the readout noise σ_R has a value of 0.5 electrons, while it appears to be possible if the readout noise σ_R is 0.3 electrons or lower.

To put our assertions on a solid mathematical ground, we need to look at the properties of readout noise in our image sensors, modelled as Gaussian probability distributions. The normalized Gaussian probability distribution $g_\sigma(x)$ with a standard deviation of σ around the mean value of zero is given by

$$g_\sigma(x) = \frac{1}{\sigma\sqrt{2\pi}} e^{\frac{x^2}{2\sigma^2}} \qquad (3\text{-}1)$$

This Gaussian is "normalized", meaning that the integral from minus to plus infinity is equal to one, i.e. the area under the Gaussian curve is equal to one.

$$\int_{-\infty}^{\infty} g_\sigma(x)\, dx = 1 \qquad (3\text{-}2)$$

More generally, the area under a normalized Gaussian probability function, integrated from a to b, is given in terms of the so-called error function erf(x):

$$\int_a^b g_\sigma(x) dx = \frac{1}{2}\left\{\mathrm{erf}\left(\frac{b}{\sigma\sqrt{2}}\right) - \mathrm{erf}\left(\frac{a}{\sigma\sqrt{2}}\right)\right\} \qquad (3\text{-}3)$$

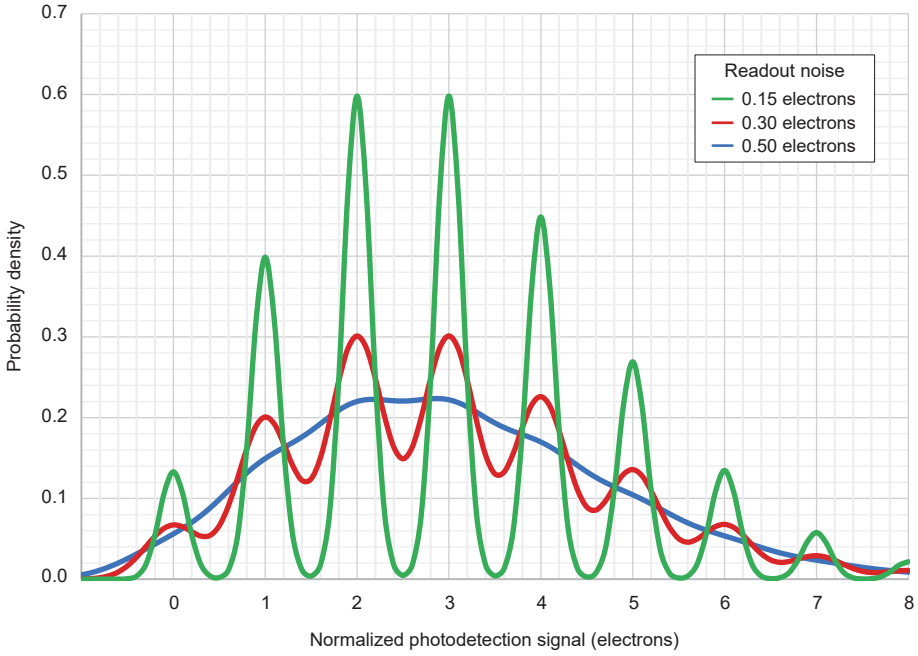

Fig. 3-1 Probability distribution of the observed photoelectrons for a Poisson distribution $P_3(k)$ with a mean of N = 3 electrons, and three different values of the readout noise: σ_R = 0.5 electrons (blue curve), σ_R = 0.3 electrons (red curve), and σ_R = 0.15 electrons (green curve).

This allows us finally to answer our question: Fig. 3-2 shows a (normalized) Gaussian probability distribution with a standard deviation σ = 0.3 electrons.

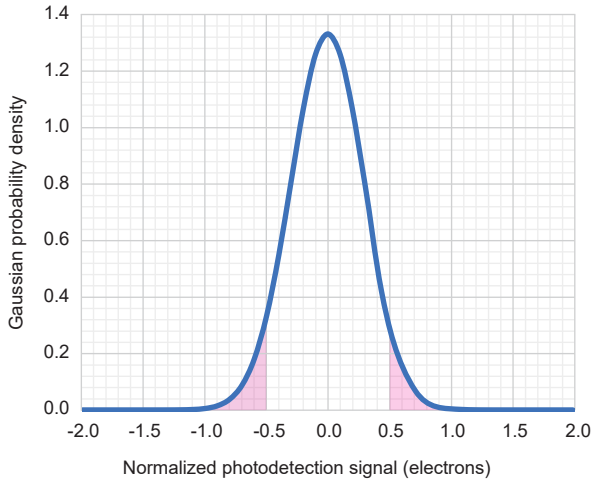

Fig. 3-2 Photosignal detection probability distribution around the mean value of N = 0 electrons, for a Gaussian distribution with σ = 0.3 electrons

The area under the Gaussian curve outside the interval [-0.5, 0.5] is shaded in red. Using equation (3-3) we can calculate this red area, i.e. the probability R(σ) that a measurement is outside the interval [-0.5, 0.5]:

$$R(\sigma) = 1 - \int_{-0.5}^{0.5} g_\sigma(x)\,dx \qquad (3\text{-}4)$$

In Fig. 3-3, this probability R(σ) is illustrated for a range of standard deviations. It can be interpreted as the probability of misclassifying an event with zero mean.

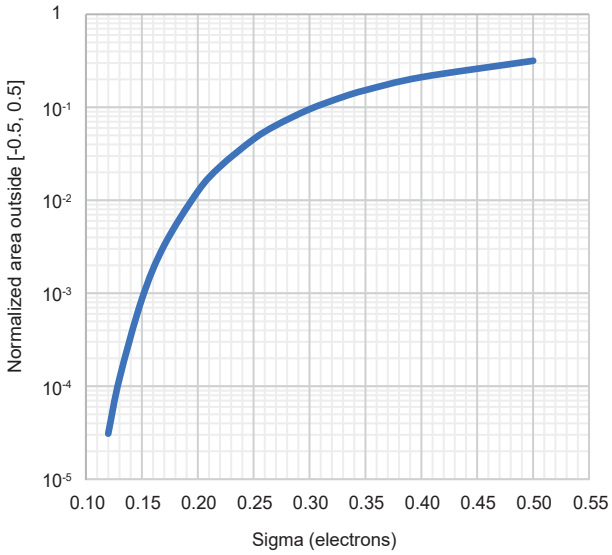

Fig. 3-3 Area outside the interval [-0.5, 0.5] of the normalized Gaussian probability distribution, indicating the probability of a misclassification of an event outside this interval

As an example, consider a standard deviation of σ = 0.5 electrons. Since R(0.5) = 0.32, this implies that in 32 % of the cases an event is misclassified as lying outside the interval [-0.5, 0.5]. If σ = 0.15 electrons then R(0.15) = 0.0009 is obtained, implying that less than 0.1 % of the events are misclassified.

It is obvious, therefore, that Gen III sCMOS technology with a readout noise larger than 0.7 electrons is insufficient for the realization of photon-resolving cameras. A new generation of CMOS image sensor technology and solid-state cameras is required.

Assuming that we demand a correct classification probability of photoelectron detection events of at least 90 %, we can conclude from Fig. 3-3 that the readout noise must be lower than σ_R = 0.3 electrons rms.

As a consequence, we call a CMOS image sensor technology “quantitative CMOS” (or qCMOS®), if it has photon number resolving capability with sufficient statistical reliability.

Not only must qCMOS® technology fulfil extreme specifications, it must be complemented by appropriate camera technology to make full use of the qCMOS® capabilities. As an example, consider one of the consequences of qCMOS® process non-uniformity: In Section 1.2.1 it was mentioned that the charge detection sensitivity of a CMOS image sensor is given by q/C. In qCMOS® technology, very small semiconductor structures are employed to implement effective input capacitances C of less than 1 fF. Since these structures are so small, it is not possible to produce them with high reliability – rather there is a spread in the obtained C and q/C values. As an example, the qCMOS® image sensor presented in [3] shows a charge detection sensitivity spread of 330 to 400 µV/e around a mean value of 368 µV/e. This implies that the signal of a single photodetection event can vary by about ± 8 % over the whole surface of such a qCMOS® image sensor. As a consequence, it is absolutely necessary to calibrate each individual pixel and to correct its signal in real-time by the camera electronics, to realize a reliable photon number resolving camera. It is also mandatory to keep essential properties of the qCMOS® image sensor and the camera stable with temperature and time, with a stability significantly below one percent.

As an example of the great care that must be taken in the implementation and use of qCMOS® image sensors, consider a pixel whose target capacitance value C is off by only one percent. As a consequence, the charge detection sensitivity is also off by one percent. Assume that the photodetection probability is a Gaussian with a standard deviation of σ = 0.3 electrons, and we would like to detect a signal consisting of N = 10 electrons. If the actual probability distribution is off by one percent, i.e. the mean signal is rather N = 10.1 electrons, then the area under the Gaussian up to 9.5 electrons is more than four times smaller than the area above 10.5 electrons. This is an inacceptable skew in the misclassification performance of such an improperly calibrated qCMOS® image sensor.

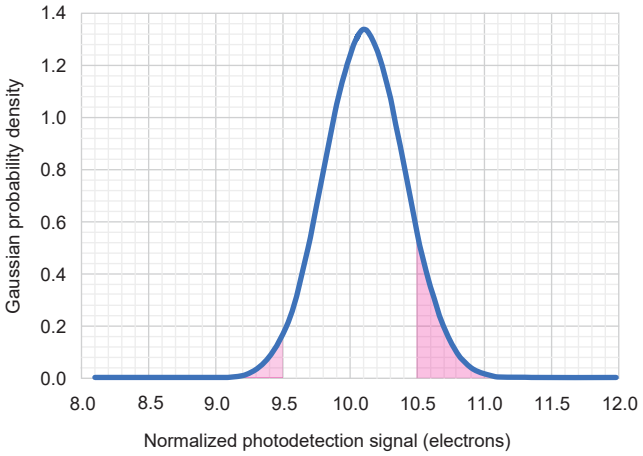

Fig. 3-4 Photosignal detection probability distribution around the mean value of N = 10.1 electrons, for a Gaussian distribution with σ = 0.3 electrons

The readout noise performance of a Gen III sCMOS image sensor of 0.7 electrons rms or more is insufficient for the realization of a true photon number resolving camera. If a correct classification of the photoelectron number for more than 90 % of the photodetection events is demanded, a readout noise of 0.3 electrons rms or less is required. This can be achieved with the most recent CMOS image sensor technology termed “quantitative CMOS” qCMOS®. The maximum performance of qCMOS® image sensors can only be unleashed in a photon number resolving camera if appropriate advanced camera technology is employed, achieving extremely high stability with temperature and time, and requiring the individual calibration and real-time correction of each pixel value.

4. Challenges for a Photon Number Resolving Camera with the Custom qCMOS® Image Sensor

Hamamatsu Photonics is developing a novel camera with a custom qCMOS® sensor called the "qCMOS® camera". Not only will the qCMOS® camera deliver the exceptional performance needed for scientific applications, but it will uniquely offer photon number resolving capability.
Some of the key features of the qCMOS® camera are introduced in this chapter.

4.1 Readout noise performance and uniformity

The qCMOS® camera will achieve excellent readout noise performance by using the latest CMOS technologies. Fig 4-1 shows that the qCMOS® camera obviously has quite narrow noise distribution with 0.19 electrons mode and 0.27 electrons rms compared to the Gen II and Gen III sCMOS technologies.

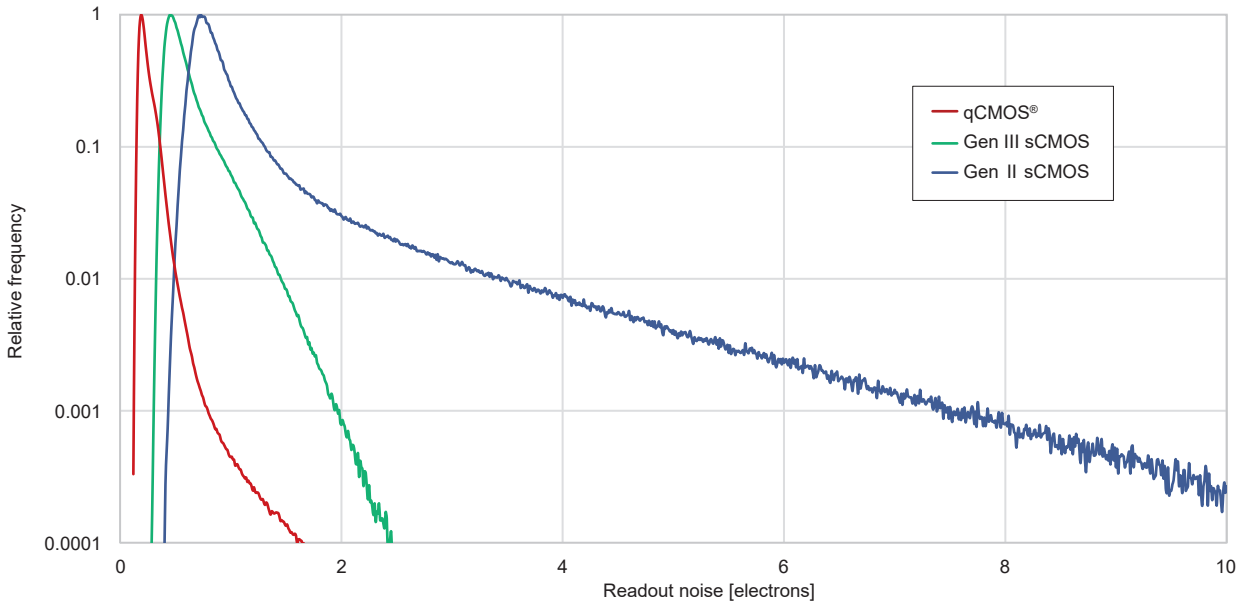

Fig. 4-1 Comparison of typical noise distributions between qCMOS®, Gen II sCMOS and Gen III sCMOS

The rSNR which is explained in section 1.3 is one of the parameters to express the performance. For example, Fig 4-2 shows the rSNR of a qCMOS® camera. When the average number of photons is 0.1 photons, the rSNR is approximately 4 times higher than those of Gen II sCMOS cameras, and it is better than the rSNR value reached with EM-CCD cameras. As a consequence, the detection limit under ultra low light conditions could be improved using the qCMOS® camera.

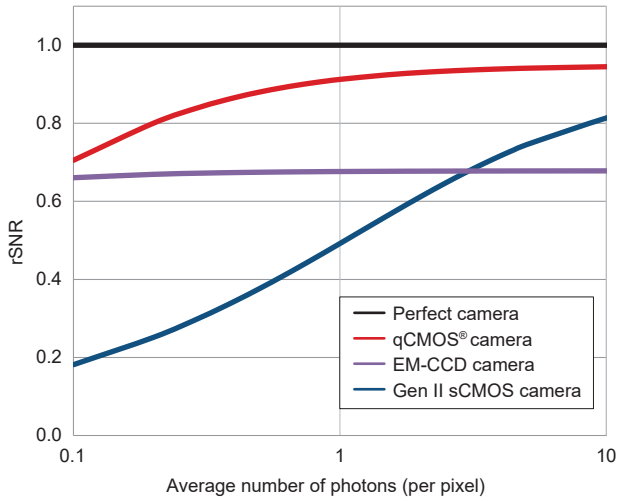

Fig. 4-2 rSNR comparison

As examples, comparisons between the qCMOS® camera and conventional cameras (Gen II sCMOS and EM-CCD cameras) are shown in Fig. 4-3 and Fig. 4-4. Fig. 4-3 shows the qCMOS® vs Gen II sCMOS camera under mean 2 photons/pixel/frame.
The image of the qCMOS® camera has much better quality compared to a Gen II sCMOS camera, due to the higher SNR of the qCMOS® camera.

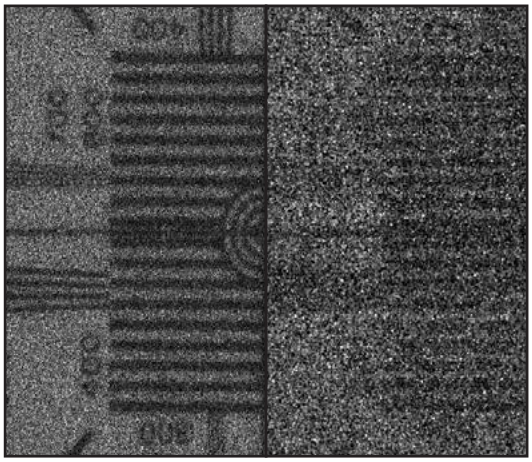

(Left) qCMOS® camera (Right) Gen II sCMOS camera

Fig. 4-3 qCMOS® camera vs Gen II sCMOS camera (mean 2 photons/pixel/frame)

Fig. 4-4 shows the qCMOS® vs EM-CCD camera under mean 1.4 photons/pixel/frame.
The image of the qCMOS® camera is quieter than that of the EM-CCD as it has the effect of “multiplication noise” as explained in chapter 2.

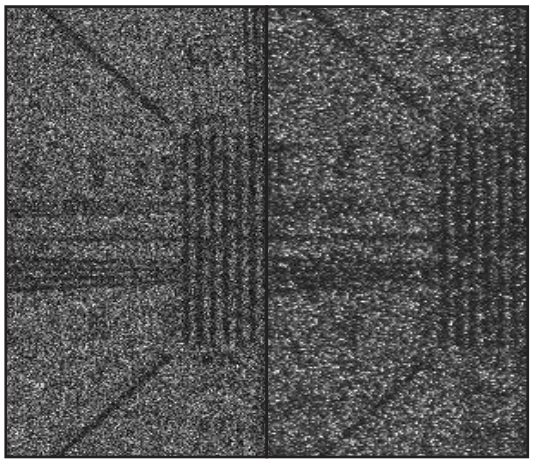

(Left) qCMOS® camera (Right) EM-CCD camera

Fig. 4-4 qCMOS® camera vs EM-CCD camera (mean 1.4 photons/pixel/frame)

4.2 Effective number of pixels

The number of pixels in conventional scientific cameras is, for example, 4.2 megapixels with 6.5 μm pixel size (Gen II sCMOS camera) or 1 megapixels with 13 μm pixel size (EM-CCD). With 9.4 megapixels, the qCMOS® camera more than doubles the pixel count of high performance Gen II sCMOS cameras.
Therefore, more high resolution imaging could be possible with the qCMOS® camera.

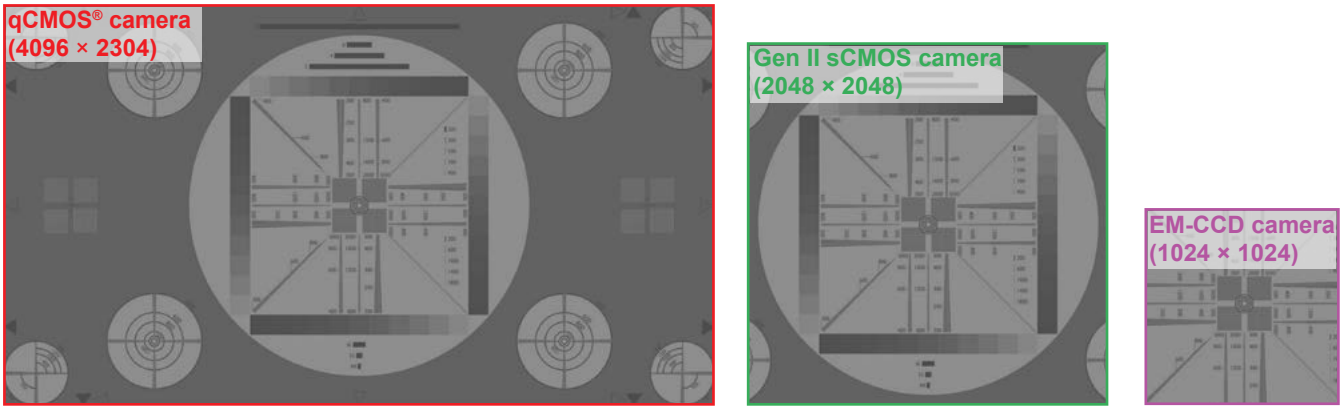

Fig. 4-5 Comparison of the number of pixels between a qCMOS® camera, Gen II sCMOS camera and EM-CCD camera

4.3 Quantum efficiency

qCMOS® image sensor technology, as shown in Fig 4-6, uses three measures to ensure maximum sensitivity:
1) BSI (Back-Side Illumination)
2) DTI (Deep Trench Isolation)
3) Microlens
Despite the small pixel size of 4.6 µm, a peak of 85 % was reached and is still 30 % at 900 nm.

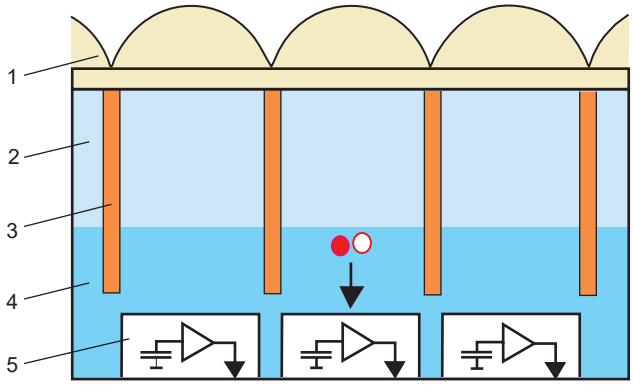

Fig. 4-6 Schematic cross section through BSI (Back-Side Illumination) qCMOS® image sensor showing DTI (Deep Trench Isolation) structures, a layer with microlenses on top.

1: Microlenses
2: Field-free region (photocharge transport through diffusion)
3: DTI (Deep Trench Isolation) structures
4: Electric field region (photocharge transport through drift)
5: Pixel structure for electronic photocharge detection

1) BSI
The image sensor is illuminated from the back surface (so-called Back-Side Illumination, (BSI)), so that the incident light does not need to pass through the partially opaque pixel structures at the surface of the semiconductor material.
In addition, the image sensor substrate is thinned down to a thickness of typically 10 µm to 20 µm, so that photogenerated charges can reach the pixels before recombination takes place and they are lost for electronic detection.

2) DTI
As explained in section 1.1, blue photons tend to be absorbed closer to the surface of the image sensor, while red (and infrared) photons tend to be absorbed at the deep region of the image sensor. Therefore, some incident red photons do not interact within a pixel and move outside of the image sensor.
Although the quantum efficiency of red photons is improved if the thickness of silicon increases, cross talk becomes worse.
This is due to photoelectrons generated in the field-free region and incident red photons arriving at an oblique angle of incidence are easier to move to neighboring pixels. This phenomenon can be significantly reduced by the technological fabrication of “mechanical dividers” between the pixels, reaching through the field-free region. This technology is called DTI, Deep Trench Isolation [9]. Some photons and photoelectrons moving to the outside of a pixel are reflected by the mechanical divider and interact with the semiconductor within the same pixel. As a consequence, the quantum efficiency of the NIR region could be improved with quite low cross talk.

3) Microlens
Applying microlens technology contributes to the improvement of QE performance as the microlens can collect photons to a pixel efficiently.

4.4 MTF

One downside of back-side illumination is increased spatial crosstalk of the pixels, which can be described by the Modulation Transfer Function (MTF). To limit the effects of spatial crosstalk, the qCMOS® camera employs DTI structures as explained in section 4.3. Fig 4-7 shows a MTF comparison at 565 nm between the qCMOS® camera and a Gen II sCMOS camera.

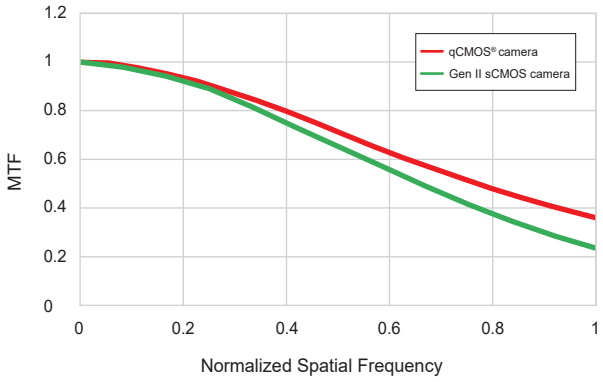

Fig. 4-7 Comparison of MTF normalized to Nyquist between a qCMOS® camera and Gen II sCMOS camera

4.5 Etaloning

Etaloning is a phenomenon that occurs when the incident light interferes with the reflected light from the back surface of the silicon and causes varying sensitivity - dependent both on the spatial and the spectral position. In the case of an EM-CCD camera, it appears as a fringe pattern even with uniform monochrome light input, mostly in the IR. The qCMOS® camera shows minimal etaloning compared to EM-CCD cameras.

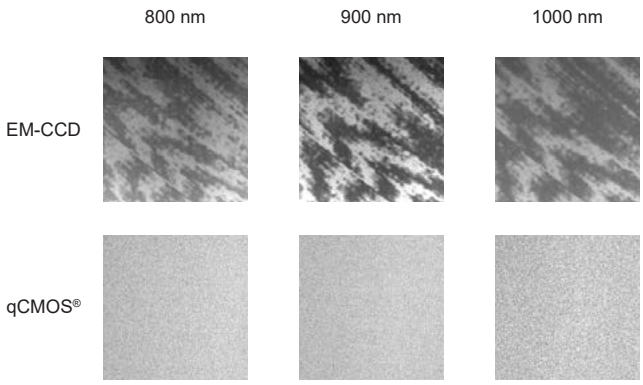

Fig. 4-8 Etaloning-desensitized

4.6 Photon number resolving mode

The qCMOS® camera will achieve 0.27 electrons rms readout noise, as shown in section 4.1. This means the qCMOS® camera has the photon number resolving capability, explained in chapter 3. In Fig. 4-9, an example of the photon number resolving capabilities is shown. The data was obtained from a single pixel, which was illuminated with a stable light source at two light intensities. More than 1000 measurements were taken (1000 "single pixel frames"). The raw data points can be seen on the left side, a cumulated and smoothed visualization of the data on the right side. As expected, a distribution resembling a Poissionian can be observed.
The qCMOS® camera is the first technology to offer photon number resolving on a multi pixel basis - in this situation even at almost 10 MP. Fig. 4-10 shows a simulated image for comparison of the qCMOS® camera in photon number resolving mode and in normal mode with the well established Gen II and EM-CCD cameras. While the EM-CCD and Gen II sCMOS cameras cannot realize photon number resolving due to multiplication noise or higher readout noise, the qCMOS® camera realizes special photon number resolving in addition to temporal photon number resolving. The camera also has a special mode called “photon number resolving mode”. It can output the digital data as a photon number (one digital number per one photoelectron) by quantifying the output digital data from the AD converter to a photon number with real time image processing. The qCMOS® camera is the first innovative camera with photon number resolving capability.

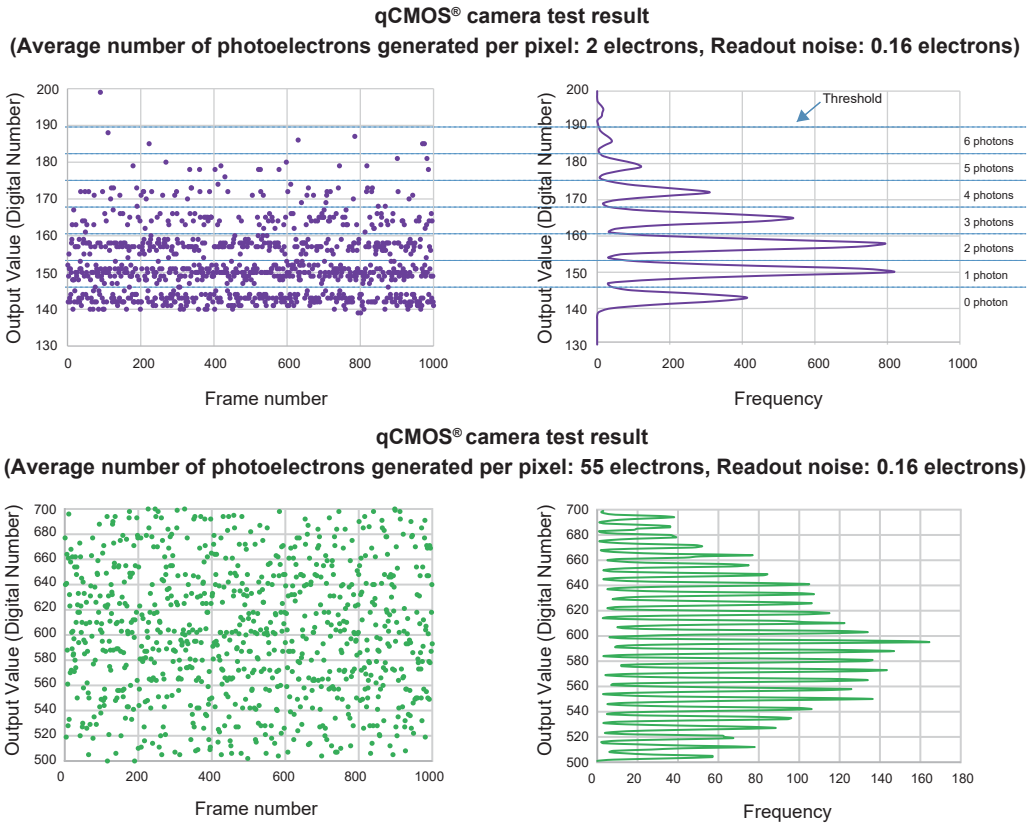

Fig. 4-9 Photon number resolving capability (Temporal)

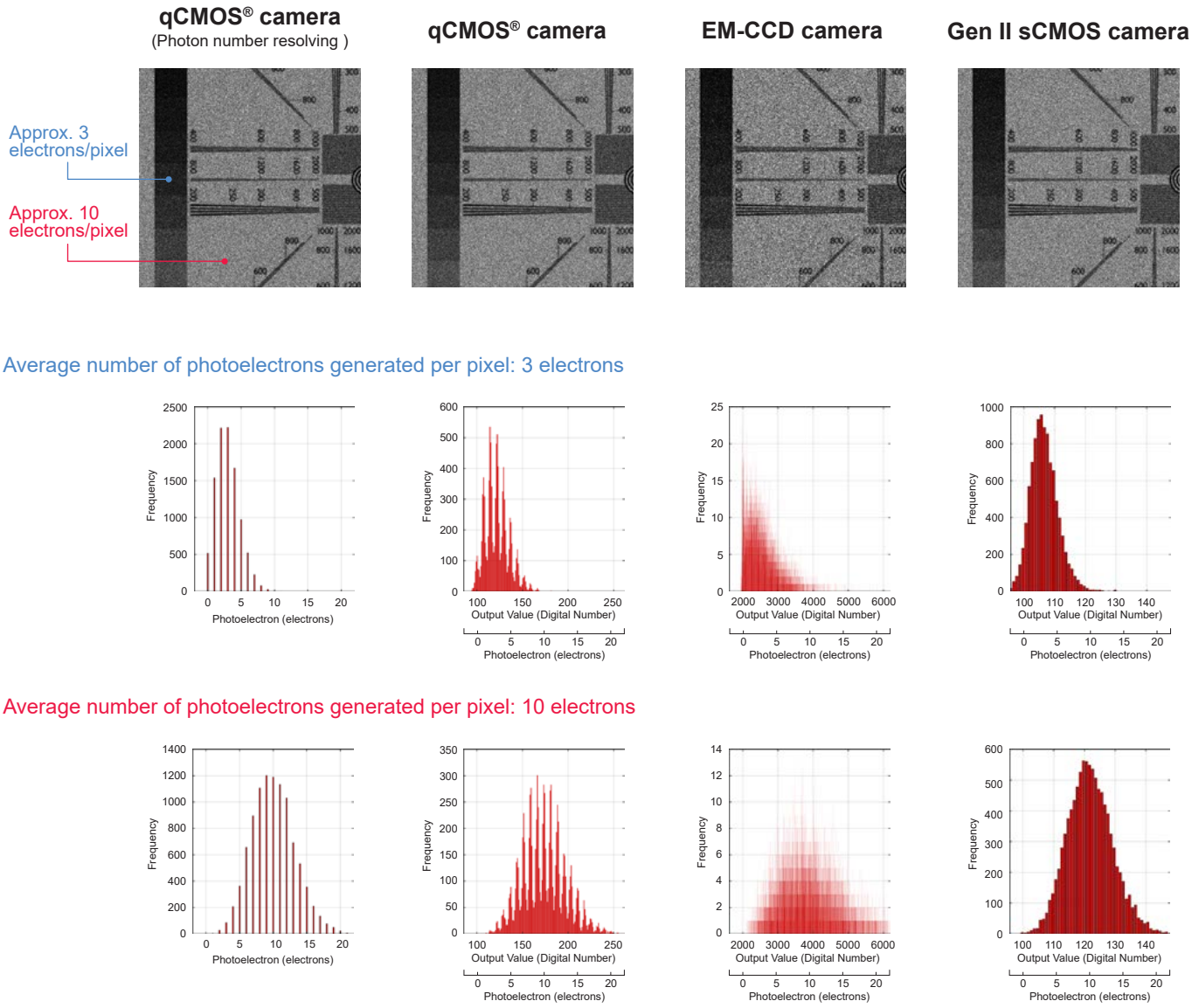

Fig. 4-10 Photon number resolving capability (Spacial)

The qCMOS® camera developed by Hamamatsu Photonics utilizes a very high performance custom qCMOS® image sensor, achieving the following specifications:

Camera Parameter	Value
Effective number of pixels	9.4 megapixels
Pixel size	4.6 μm × 4.6 μm
Quantum efficiency	85 % (460 nm) ; 30 % (900 nm)
Readout noise	0.27 electrons rms
Spatial cross talk (MTF)	Improved by DTI technologies
Etaloning	Desensitized
Photon number resolving	Available

Summary

Since the 1980s, Hamamatsu Photonics has been developing high-performance cameras for a diverse range of scientific applications.

Our primary goal was to achieve the ultimate performance in quantitative measurement in the development of our image sensors and cameras.

In 2021, we are proud to announce the release of the world's first photon number resolving camera which employs our ground-breaking qCMOS® image sensors.

We can now offer you the 'Holy Grail' of quantitative measurement, allowing you to unlock the next chapter in your scientific research, where photon number resolving is key.

References

1 A. Einstein, “Über einen die Erzeugung und Verwandlung des Lichts betreffenden heuristischen Gesichtspunkt ” , Annalen der Physik Vol. 17, 132 (1905)

2 P. Seitz, “Fundamentals of Noise in Optoelectronics”, in “Single-Photon Imaging”, P. Seitz and A. Theuwissen (Eds.), Springer, Berlin (2011).

3 J. Ma, S. Masoodian, D.A. Starkey and E.R. Fossum, “Photon-number-resolving megapixel image sensor at room temperature without avalanche gain”, Optica Vol. 4 (2017)

4 P. Seitz, “Single-Photon Imaging”, Proceedings of the International Image Sensor Workshop IISW-2011, Hakodate, Japan (2011)

5 L. Li et al., “Assessing low-light cameras with photon transfer curve method”, Journal of Innovative Optical Health Sciences, Vol. 9, 2016

6 M. Riordan and L. Hoddeson, “Crystal Fire”, W.W. Norton & Co., New York (1997)

7 E.R. Fossum, “Active Pixel Sensors: Are CCDs dinosaurs?” in Proc. SPIE CCD’s Optical Sensors III, vol. 1900 (1993)

8 J. Hynecek, “Impactron—A New Solid State Image Intensifier”, IEEE Transactions on Electron Devices, Vol 48 (2001)

9 Y. Kim et al., “A 1/2.8-inch 24Mpixel CMOS Image Sensor with 0.9μm Unit Pixels Separated by Full-Depth Deep-Trench Isolation”, Proceedings of the IEEE International Solid-State Circuits Conference ISSCC-2018 (2018)

NOTE

NOTE

NOTE

Contact information

HAMAMATSU PHOTONICS K.K., Systems Division
812 Joko-cho, Higashi-ku, Hamamatsu City, 431-3196, Japan
Telephone: (81)53-431-0124, E-mail: export@sys.hpk.co.jp

Hamamatsu Corporation
360 Foothill Road, Bridgewater, NJ 08807, U.S.A.
Telephone: (1)908-231-0960

Hamamatsu Photonics Deutschland GmbH
Arzbergerstr. 10, 82211 Herrsching am Ammersee, Germany
Telephone: (49)8152-375-0, E-mail: info@hamamatsu.de

More information on Hamamatsu scientific cameras is available at
https://camera.hamamatsu.com

Cat. No. SCAS0149E02
NOV/2023 HPK
Created in Japan